Biochemical and Biophysical Research Communications 554 (2021) 131–137

Contents lists available at ScienceDirect

Biochemical and Biophysical Research Communications

journal homepage: www.elsevier.com/locate/ybbrc

A sub-population of *Dictyostelium discoideum* cells shows extremely high sensitivity to cAMP for directional migration

Daisuke Ohtsuka [a], Nobutoshi Ota [b], Satoshi Amaya [b], Satomi Matsuoka [a, c, d, *], Yo Tanaka [b], Masahiro Ueda [a, c, **]

[a] *Laboratory of Single Molecule Biology, Graduate School of Science and Graduate School of Frontier Biosciences, Osaka University, 1-3 Yamadaoka, Suita, Osaka, 565-0871, Japan*
[b] *Laboratory for Integrated Biodevice, Center for Biosystems Dynamics Research (BDR), RIKEN, 1-3 Yamadaoka, Suita, Osaka, 565-0871, Japan*
[c] *Laboratory for Cell Signaling Dynamics, BDR, RIKEN, Suita, Osaka, 565-0871, Japan*
[d] *PRESTO, JST, Suita, Osaka, 565-0871, Japan*

ARTICLE INFO

Article history:
Received 16 March 2021
Accepted 17 March 2021
Available online 27 March 2021

Keywords:
Chemotaxis
Microfluidic device
cAMP
Dictyostelium discoideum

ABSTRACT

The chemotaxis of *Dictysotelium discoideum* cells in response to a chemical gradient of cyclic adenosine 3′,5′-monophosphate (cAMP) was studied using a newly designed microfluidic device. The device consists of 800 cell-sized channels in parallel, each 4 μm wide, 5 μm high, and 100 μm long, allowing us to prepare the same chemical gradient in all channels and observe the motility of 500–1000 individual cells simultaneously. The percentage of cells that exhibited directed migration was determined for various cAMP concentrations ranging from 0.1 pM to 10 μM. The results show that chemotaxis was highest at 100 nM cAMP, consistent with previous observations. At concentrations as low as 10 pM, about 16% of cells still exhibited chemotaxis, suggesting that the receptor occupancy of only 6 cAMP molecules/cell can induce chemotaxis in very sensitive cells. At 100 pM cAMP, chemotaxis was suppressed due to the self-production and secretion of intracellular cAMP induced by extracellular cAMP. Overall, systematic observations of a large number of individual cells under the same chemical gradients revealed the heterogeneity of chemotaxis responses in a genetically homogeneous cell population, especially the existence of a sub-population with extremely high sensitivity for chemotaxis.

1. Introduction

The cellular phenomenon in which a cell undergoes directional movement in response to a chemical gradient is called chemotaxis. It plays important physiological roles including environmental searching in unicellular organisms and wound repair, immune response and morphogenesis in multicellular organisms [1,2]. In natural environments with complexity, the chemical gradient is not always simple, and its concentration and steepness can vary greatly. How wide is the concentration range over which the cells can exhibit chemotaxis? How do chemotactic behaviors change in response to the steepness of the gradient? How did cells evolve chemotaxis properties to survive as a species? Answering these questions will help us understand the physiological roles of chemotaxis in the survival strategies of living organisms. To that end, a systematic analysis of chemotaxis is required to reveal the responsiveness of individual cells in a population to various stimulations.

The social amoebae *Dictyostelium discoideum* is a well-established model organism for the study of eukaryotic chemotaxis mechanisms [2]. *Dictyostelium* cells exhibit remarkable chemotaxis to cAMP for aggregation in their life cycle [3,4]. During the aggregation, cAMP gradients are self-organized and relayed between multiple cells like the propagation of a wave, the so-called cAMP wave. Extracellular cAMP triggers chemotaxis by the individual cells, causing a coordinated movement sometimes in more than 100,000 cells to form one multicellular aggregate. Owing to

Abbreviations: cAMP, cyclic adenosine 3′,5′-monophosphate; PDMS, polydimethylsiloxane; PIP3, phosphatidylinositol 3,4,5-trisphosphate.

* Corresponding author. Laboratory of Single Molecule Biology, Graduate School of Science and Graduate School of Frontier Biosciences, Osaka University, 1-3 Yamadaoka, Suita, Osaka, 565-0871, Japan.
** Corresponding author. Laboratory of Single Molecule Biology, Graduate School of Science and Graduate School of Frontier Biosciences, Osaka University, 1-3 Yamadaoka, Suita, Osaka, 565-0871, Japan.
E-mail addresses: matsuoka@fbs.osaka-u.ac.jp (S. Matsuoka), masahiroueda@fbs.osaka-u.ac.jp (M. Ueda).

https://doi.org/10.1016/j.bbrc.2021.03.095

the synchronized developmental process, a highly homogeneous cell population can be prepared for the study of chemotaxis. Also, since the cAMP wave varies over a concentration range from sub-nM to 10 μM, *Dictyostelium* cells provide a model for investigating chemotactic signalling over a 10^5-fold range [5–7]. Besides these physiological advantages, *Dictyostelium* cells have general advantages for study of the molecular and cellular biology of chemotaxis: the molecular mechanisms are best understood experimentally and theoretically [2,8–11]. For example, G protein-coupled cAMP receptor, cAR1, and the cognate heterotrimeric G protein $G\alpha_2$-$G\beta\gamma$ are essential for chemotactic signalling. The cAMP receptors activate, recruit, and capture G proteins for wide-range chemotaxis, which are regulated by distinct cAMP concentrations with EC_{50} of 2.3 nM, 12 nM and 270 nM, respectively [12], suggesting that multiple signalling modes cover a wide chemotactic range. To link the molecular properties of the chemotactic signalling system to cellular directional migration, however, we need an assay for the systematic analysis of the chemotaxis of individual cells under precisely controlled signal inputs over a wide range of concentrations.

Various chemotaxis assays have been developed to apply chemical gradients to *Dictysotelium* cells. The two drop assay has been widely used to measure chemotaxis efficiency [13,14]. Here, two droplets of a cell suspension and cAMP solution are placed in close proximity on an agar plate to generate a concentration gradient around the cells. Using this assay, Mato et al. (1975) reported a threshold gradient of 3.6 pM/μm at 4.3 nM cAMP for chemotaxis [14]. While this method is simple and has the advantage of being able to measure a wide range of concentrations at once, it does not provide information on the chemotaxis ability of individual cells and thus the cellular heterogeneity in the population. In order to observe the chemotactic movement of individual cells, a glass capillary filled with attractant solution is used to generate the chemical gradient [15,16]. This assay is also simple, but it is difficult to obtain a large amount of data to analyze statistically the motility of individual cells under the same gradient conditions. In another assay, Fisher et al. (1989) prepared two semipermeable hollow fibers embedded in parallel in a thin agarose gel to generate stable chemical gradients between them over 1000 μm long [5]. The motility of individual cells can be followed under the stable gradients. Using this assay, they found that *Dictysotelium* cells can exhibit chemotaxis over a 10^5-fold range with only a 2% difference between the two ends of individual cells [5]. Song et al. (2006) utilized microfluidics techniques to generate stable linear chemical gradients over 300 μm long by continuous flow through a channel [17]. By tracking individual cells in the gradient, the threshold for chemotaxis was determined to be 3.3 pM/μm at 0.5 nM cAMP. These two assays are powerful for observing individual cells under stable gradients. However, the chemical gradient is much larger than the size of the cells and is different for cells depending on the cell location in the gradient field. Moreover, the chemotaxis efficiency can be obtained only by averaging the whole cell population.

To study single cells, here we report a microfluidic device for chemotaxis assays. The device consists of 800 cell-sized channels in parallel using microfluidics techniques, allowing us to analyze 500–1000 individual cells under the same chemical gradient in one experiment. The chemotaxis efficiency was determined by counting the number of cells moving directionally through the parallel channels in an all-or-none manner. Using this device, we found that a small number of cells are chemotactic even at extremely low cAMP concentrations of 1–10 pM, which is a range lower than those used in previous studies. Sub-populations with extremely high sensitivity to the cAMP gradient may have a critical role in aggregation for the survival of *Dictyostelium discoideum* cells.

2. Materials and methods

2.1. Preparation of the microfluidic device for the observation of chemotaxis

Fig. 1 shows a schematic diagram of the microfluidic device used in this study. The device consists of a polydimethylsiloxane (PDMS) substrate, a cover glass, and silicone tubes. The microchannels on the PDMS substrate were fabricated using the replica molding method as described previously [18,19]. The PDMS substrate has grooves 4 μm wide and 5 μm high carved into its surface (blue shape shown in Fig. 1A). When the substrate is attached to a cover glass (C024241, MATSUNAMI), the grooves form a flow channel between the mold and coverglass. The overall shape is symmetrical, with a pair of large flow channels from 3 inlets to one outlet and a ladder-like arrangement of 800 narrow channels connecting the two flow channels (Fig. 1B). Each narrow channel is 4 μm wide, 5 μm high, and 100 μm long. By flowing two solutions of different compositions from the left and right sides, they can mix in the narrow channels to form a chemical gradient. Accordingly, a cell suspension and cAMP solution were introduced into the device through the left and right inlets, respectively, and the cells moved from left to right in the narrow channels when they exhibited chemotaxis.

2.2. Microscopy and image data analysis

A confocal laser microscopy system consisting of a Nikon Eclipse Ti equipped with Yokogawa CSU-W1 and Hamamatsu ORCA-flash 4.0 CCD camera was used with a Plan Apo 60 × /1.40 NA objective lens for the image acquisition of cells in the microfluidic device. The microscope stage could be moved in both the *x*- and *y*-axes using a motorized controller (MCL nano-drive). All 800 channels in the device can be captured in 48 fields of view within 13 s, by which the multipoint measurement of the 48 fields of view was repeated every 30 s for time-lapse imaging. Fluorescein in the cAMP solution and Histone2B-RFP were excited by 488-nm and 561-nm lasers, respectively, to analyze the concentration gradient and the cell position in each field of view.

To determine the chemotaxis efficiency of the cells, cell nuclei were labeled fluorescently by introducing Histone2B-RFP, and the fluorescent images were taken as described above. The images were processed by an adaptive binarization method to extract the cell nucleus, and the centroid of the nucleus was calculated as an index of the cell position. The cells on the right side of the channel center were defined as cells attracted to cAMP. The chemotaxis efficiency was calculated by dividing the total number of attracted cells by the total number of all cells in the 48 fields of view.

2.3. Cell preparations and other methods

Full methods and any associated references are available in the supplementary information.

3. Results

3.1. Chemotaxis of Dictyostelium cells in a stable cAMP gradient generated by the microfluidic device

We examined how the chemical gradient actually forms in the device. A buffer (DB) and 100 μM fluorescein-containing DB were flowed into the left and right channels of the device, respectively, and the fluorescence intensity in the device was measured every 30 s for 1 h. Fig. 1C shows a typical microscopic image. When the fluorescent dye started to flow at time 0 min, the gradient started to

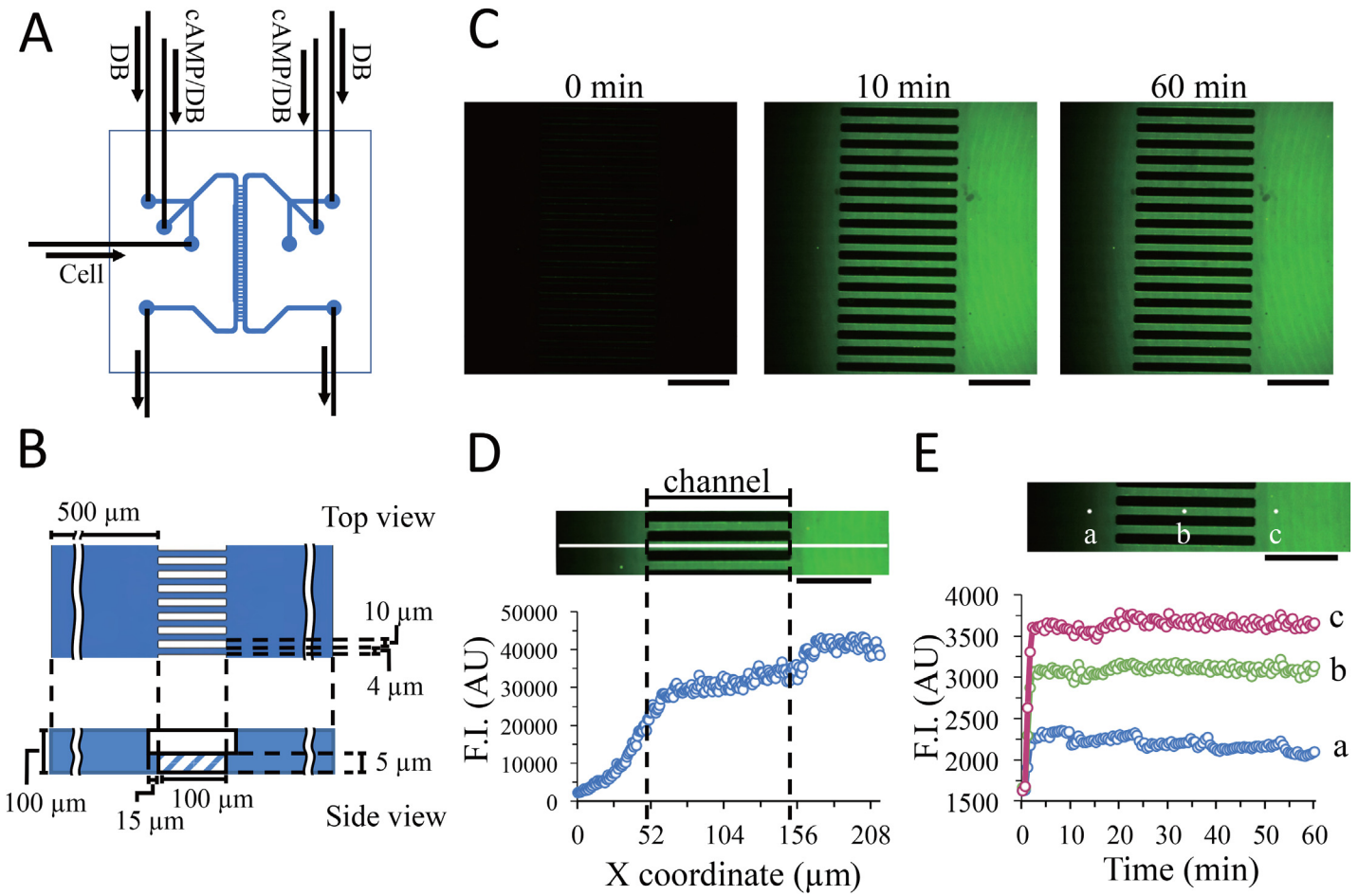

Fig. 1. Schematic diagram of the microfluidic device and evaluation of the concentration gradient. (**A**) Layout of the device. The device has six inlets, two outlets and 800 narrow channels in parallel between the two flow channels. (**B**) An illustration of the channels. Top and side views are shown above and below, respectively. A single narrow channel is 4 μm wide, 5 μm deep, and 100 μm long. (**C**) A gradient of 100 μM fluorescein flowing in the channel. Scale bars, 50 μm. (**D**) Fluorescence intensity plot from the white line in the upper image taken 10 min after the fluorescent dye started to flow. Scale bar, 50 μm. (**E**) Time course of the fluorescence intensity at points **a**, **b**, and **c** shown in the upper image. Scale bar, 50 μm.

form within 2 min and continued for at least 1 h. The fluorescence intensity was measured at the location indicated by the white line in the upper image of Fig. 1D, showing that a shallow gradient was formed in the narrow channel, while a steep gradient was formed within a distance of 30 μm to the left side of the channel. The temporal changes in the fluorescence intensities at the three locations shown in Fig. 1E were measured for 60 min and show that the intensities reached steady state in 2 min and was almost constant thereafter for 60 min. Thus, we confirmed the formation of a stable gradient. Both the entrance and inside of the narrow channels have spatial scales that are not significantly different from the cell size, thus, the cells can be stimulated along the 800 parallel channels by a chemoattractant gradient in the same way.

We next observed the response of *Dictyostelium* cells to cAMP gradients formed using the microfluidic device. Cells were introduced into the left side of the narrow channel, and then 10^{-7} M cAMP solution was pumped into the right flow channel to initiate the formation of the cAMP gradient (Fig. 2A, left, time = 0 min). The cell nuclei were fluorescently labeled with Histone2B-RFP to facilitate analysis of the cell motility, and 100 μM fluorescein was mixed with the cAMP solution to confirm that a stable gradient was formed. Time-lapse imaging of Histone2B-RFP and fluorescein was performed simultaneously using a confocal laser microscope. Immediately after the formation of the concentration gradient, we observed that some cells entered the narrow channel and started to migrate directionally to the right. In the first 20–30 min, cells entered the narrow channel one after another, and they progressed through the channel toward the cAMP side, while the rest of the cells remained in the original left channel. It was often observed that cells within 50 μm of the left side of the narrow channel entered the channel. After 60 min, most of the cells had migrated through the channel to the right side (Fig. 2A), while the cells that remained at the left rarely migrated to the right even after more time had elapsed. These results indicate that the microfluidic device fabricated in this study can be used to analyze the chemotaxis response of *Dictyostelium* cells to cAMP. Because this device can generate the same concentration gradient everywhere in the 800 channels, whether individual cells could or could not respond to the same concentration gradient in the cell population could be identified. Also, even among cells that could respond to the cAMP gradient, there was a mixture of cells that started chemotaxis shortly after the stimulation and those that started after a longer lag.

To analyze how the chemotaxis response changes over a wide range of cAMP concentrations, we considered introducing an index to quantify the chemotaxis efficiency at a given concentration. As described above, the cells entered the narrow channel from the left side and continued to move to the right direction. Once they entered the flow channel on the right side, they rarely re-entered the narrow channel from the right side and moved backward. We therefore counted the cells on the right side of the narrow channel and defined chemotaxis efficiency as the percentage of the total number of cells. Thus, the chemotaxis response of individual cells is evaluated in an all-or-none manner, and the obtained chemotaxis efficiency indicates the percentage of cells that showed chemotaxis in the total cell population. Fig. 2B shows the temporal change in

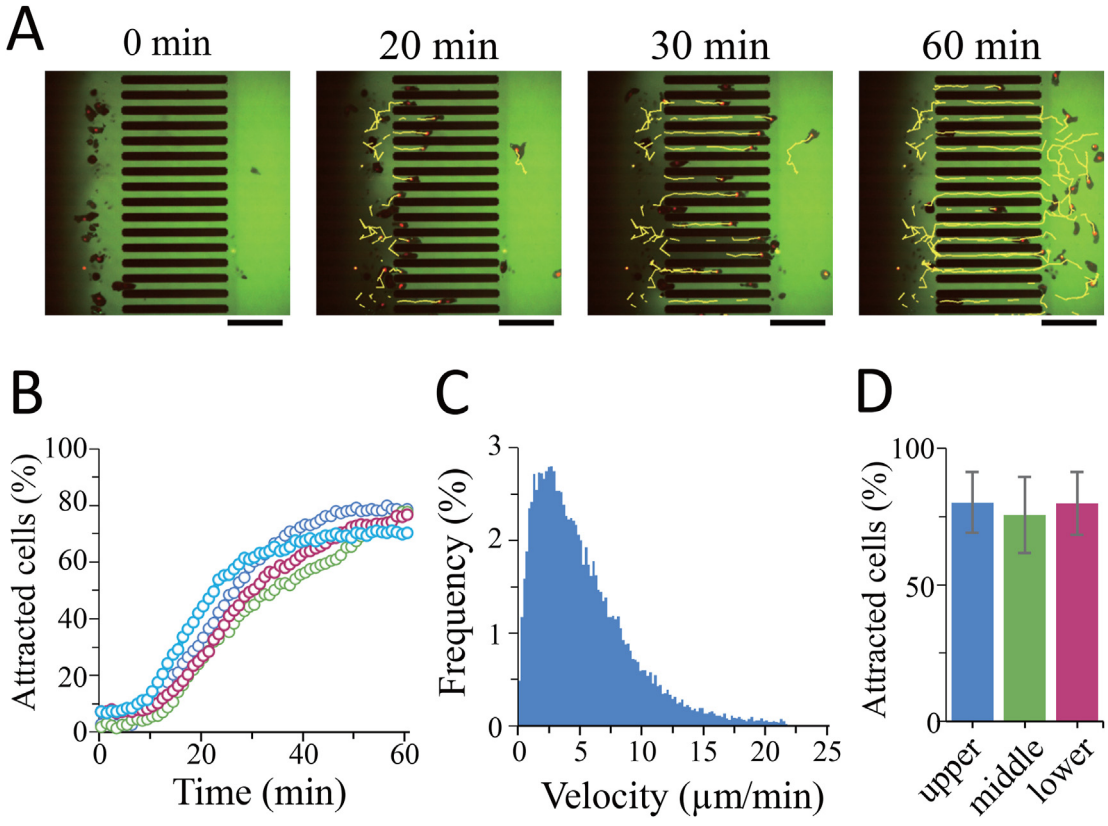

Fig. 2. Chemotaxis of *Dictyostelium* cells in the microfluidic device. (**A**) Images of cells attracted to 100 nM cAMP. When the cAMP-containing solution was flowed, a gradient was formed within 2 min. The time of the gradient formation was set to 0, and the cells were observed and tracked using a confocal laser microscope to obtain the trajectories (yellow lines). Red, Histone2B-RFP; green, fluorescein. Scale bars, 50 μm. (**B**) Time course of the percentage of cells that moved toward cAMP from 4 independent experiments. (**C**) The distribution of velocities of cells in the narrow channels. Cell trajectories were obtained in 30-sec intervals, and the centroids of the Histon2B-RFP signals were used to calculate the velocity ($n = 26746$ data points from 750 cells). (**D**) Chemotaxis efficiency in the upper (blue), middle (green), and lower (purple) 16 channels. (For interpretation of the references to colour in this figure legend, the reader is referred to the Web version of this article.)

the chemotaxis efficiency after the gradient formation with 100 nM cAMP. The time series varied somewhat from experiment to experiment in both the lag-time when the percentage started to increase and the rate of the increase. Regardless, the chemotaxis efficiency reached a roughly constant value after 60 min. We thus decided to use this value as an index reflecting the chemotaxis response under a given cAMP concentration. The velocity of cell migration in the narrow channel was 5.2 ± 3.9 μm/min ($n = 26746$ data points from 750 cells), consistent with previous observations (Fig. 2C) [5,17].

To confirm the cell response to cAMP across the entire narrow channel in the device, all 800 channels were observed in 48 separate fields of view, the chemotaxis efficiency was determined in each field of view, and the mean and standard deviation of the chemotaxis efficiency were calculated for three separate 16 fields of view. As shown in Fig. 2D, there was no significant difference in the chemotaxis efficiency among the three regions, meaning that the cells showed a similar and reproducible response in this device across the entire channel. To track the movement of individual cells reliably, the number of cells in one field of view was set to about 10–20 maximum. Thus, the chemotaxis response of about 500–1000 cells can be measured using this device in one experiment.

3.2. Chemotaxis of Dictyostelium cells over a wide range of cAMP concentrations

We next characterized the dependence of chemotaxis on the cAMP concentration. We determined the chemotaxis efficiency for various cAMP concentrations ranging from 0.1 pM to 10 μM, as shown in Fig. 3A. In the absence of cAMP, the chemotaxis efficiency was 14.9 ± 3.4%, indicating the percentage of cells that reached the right half region of the narrow channel within 60 min by spontaneous migration. There was no increase in the chemotaxis efficiency at 10^{-13} M cAMP compared to the control, showing no chemotaxis in this condition. In the concentration range 10^{-12}–10^{-11} M, the cells migrated toward the cAMP solution significantly compared to the control. The highest percentage was obtained at 10^{-7} M cAMP, in which the half-maximum response was observed around sub-nM cAMP. These results are roughly consistent with previous studies showing that the chemotaxis range of *Dictyostelium* cells is approximately 10^{-10} to 10^{-6} M [5]. On the other hand, we noticed that some cells showed chemotaxis even at 10^{-11} M cAMP, a concentration at which chemotaxis was hardly detected in previous studies. When we observed individual cells in the narrow channel, we found that the cells tended to continue moving to the right at 10^{-7} M cAMP, but they often exhibited back and forth migration as the cAMP concentration decreased. That is, even for cells that could respond to very low cAMP concentrations, the persistence of cell movement toward the attractant was lower than at higher concentration ranges. This minority of cells with high sensitivity may be buried when the data is averaged over the whole cell population. Thus, this assay using the microfluidic device detected the existence of sub-populations of cells with extremely high sensitivity to very low attractant concentrations.

We noticed that the concentration dependency curve shown in Fig. 3A was apparently bimodal with a valley-like appearance at 10^{-10} M. One possible reason for this is that the chemotactic signalling pathway has a unimodal dependence with a peak at 10^{-7} M, but some secondary response causes the bimodal effect. The threshold concentration of external cAMP that causes the self-production and secretion of intracellular cAMP is about 0.5 nM [20], which is of the same range detected in this study. Such

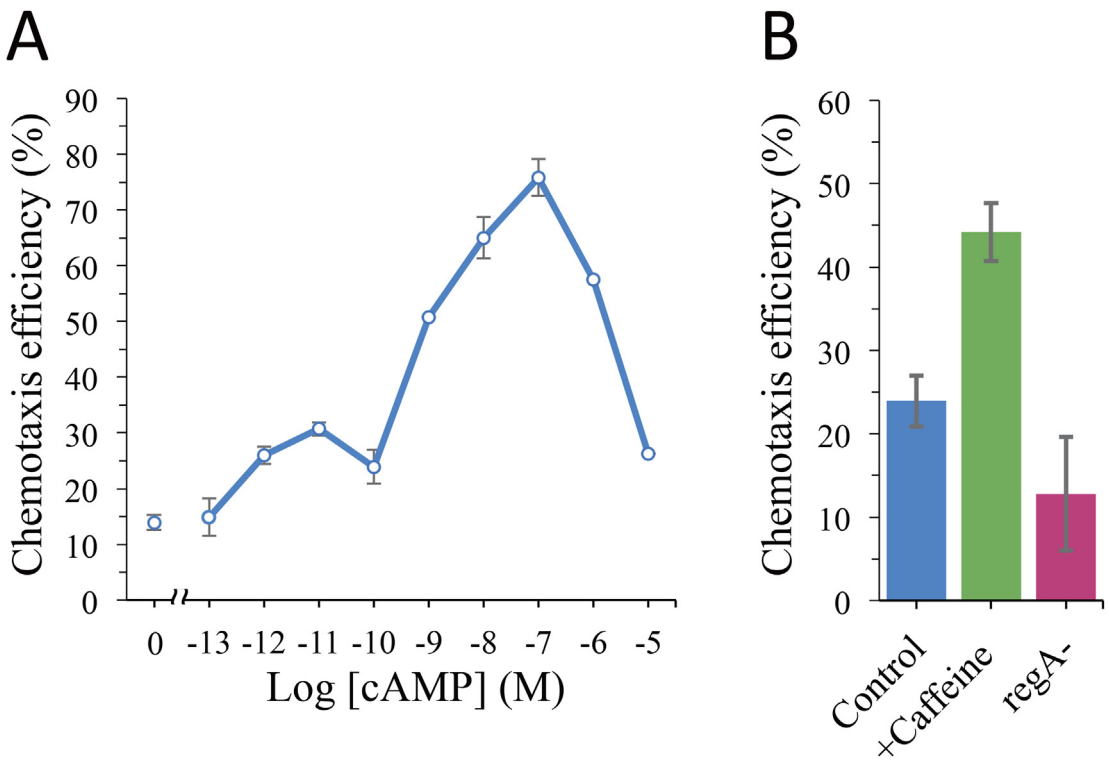

Fig. 3. Dependence of chemotaxis on cAMP concentration. (**A**) Chemotaxis efficiency of *Dictyostelium* cells in 0.1 pM–10 μM cAMP. Data were obtained from one to four independent experiments with approximately 500–1000 cells observed in each experiment and represent the mean ± SE. (**B**) Effects of the self-production of cAMP in chemotaxis. Chemotaxis efficiency at 0.1 nM was measured in control (blue), caffeine-treated (green) and *regA*-knockout (red) cells. Chemotaxis efficiency was obtained from 3 independent experiments. Data represent the mean ± SE. (For interpretation of the references to colour in this figure legend, the reader is referred to the Web version of this article.)

external cAMP-induced cAMP secretion may cause the disappearance of the gradient at 10^{-10} M. To test this hypothesis, we modulated the cAMP synthesis and secretion pathways in two ways. First, cAMP synthesis was inhibited with 4 mM caffeine [21], and the chemotaxis efficiency was determined. As a result, the chemotaxis efficiency increased to 44.2 ± 3.5% by caffeine treatment ($n = 1109$ cells) compared to 23.9 ± 3.1% without the treatment ($n = 2399$ cells) (Fig. 3B). We next examined the chemotaxis efficiency in a strain lacking the gene for RegA (*regA*$^-$), a phosphodiesterase responsible for cAMP degradation in the cell [22]. We found that 12.8 ± 6.8% of *regA*$^-$ strain cells responded ($n = 2036$ cells). These results indicate that chemotaxis at 10^{-10} M cAMP was suppressed by cAMP section by the cells themselves, meaning that the cells have sufficient ability to sense the chemical gradient even at 10^{-10} M cAMP.

4. Discussion

In this study, we developed a microfluidic device with 800 channels in parallel for chemotaxis assays to apply the same chemical gradients to 500–1000 cells in a single experiment (Fig. 1). The chemotaxis response of individual cells can be judged in an all-or-none manner and is not averaged over the population (Fig. 2). Thus, this assay can detect the subpopulations responsive under a given concentration gradient. As a result, a small number of cells capable of showing chemotaxis was detected even at very low cAMP concentrations (10^{-11} M) (Fig. 3).

Based on the receptor binding kinetics [23], we estimated the number of cAMP molecules bound to cells at 10^{-11} M cAMP. To calculate the receptor occupancy, we consider the simplest reaction scheme, $R + cAMP \leftrightarrow R^*$, where R and R* are a cAMP receptor in free and occupied form, respectively. Then, the receptor occupancy in a single cell is given by Michaelis-Menten kinetics,

$$R^* = \frac{[cAMP]}{K_D + [cAMP]} R_{total}$$

where *Rtotal* is the total number of receptors per cell, K_D is the cAMP-binding affinity, and [*cAMP*] is the cAMP concentration. Previous studies have shown at least two states of affinity for the cAMP receptor: high affinity at 10 nM cAMP and 3400 receptors per cell, and low affinity at 300 nM cAMP and 77000 receptors per cell [23]. Thus, the receptor occupancy can be calculated for a given cAMP concentration in nM as follows,

$$R^* = \frac{[cAMP]}{10 + [cAMP]} 3400 + \frac{[cAMP]}{300 + [cAMP]} 77000$$

When the cAMP concentration is 10^{-11} M, the receptor occupancy in a single cell is estimated to be 6 molecules on average. Even if a sensitive cell has twice the number of receptors, the estimated value is 12, which is still a small number. Finally, even if the stimulus given to the cell is localized, the steady-state binding of up to 6–12 molecules of cAMP per cell determines the cellular chemotactic behavior.

In this device, a steep gradient of cAMP is formed on the left side of the narrow channel, and a shallow gradient is formed inside the channel (Fig. 1). From the fluorescence intensity obtained experimentally, the cAMP gradient was calculated to be 10% over 100 μm in the narrow channel. If we assume that the cell length is 20 μm in the channel, then the cell senses a concentration difference of about 2%. It is known that *Dictyostelium* cells can bias their motility toward cAMP in a 2% gradient [5,14,17], thus, we assumed that the cells in the channel also sensed the gradient. In fact, reversing the gradient direction could cause the cells in the narrow channel to reverse their migration direction. However, it is also possible that cell polarity or the self-generation of a cAMP gradient can contribute to the directional movement in the channel. *Dictyostelium* cells show anterior-posterior polarity in response to cAMP and can form pseudopods at the anterior side more efficiently even when they are exposed to a uniform cAMP solution [15]. In our device, the cells were polarized in the direction of cAMP at the time they entered the channel, which may give rise to a tendency for continuous movement in the direction of the cAMP in the channel. In addition, recent studies have shown that *Dictyostelium* cells are able to generate their own gradient toward a cAMP source by degrading nearby cAMP [24]. This ability may help to form a sustained unidirectional movement in the narrow channel. At the entrance of the narrow channel, the cells could sense a steep gradient, in which the maximum concentration does not exceed the given cAMP concentration. At the threshold stimulation for chemotaxis, 10^{-11} M cAMP with a steep gradient could induce cells to enter the narrow channel.

The chemotaxis of *Dictyostelium* cells has the characteristic feature of an excitable system [2,10,11,25,26]. Even in the absence of cAMP, excitable systems stochastically generate Ras and PIP3 domains, which act as signals to regulate pseudopodia, leading to spontaneous cell migration [25–27]. This spontaneous signal generation is probably due to molecular noise generated intrinsically in the excitable system [10,26,28]. The system also triggers chemotaxis in response to cAMP gradients. One likely reason why *Dictyostelium* cells can respond to very small signal inputs is that the excitable system functions as a signal amplifier. However, the system can also amplify small random noises in the input signal, which would randomize cell migration. Indeed, chemotaxis efficiency is sensitive to molecular noise [16,29–31]. Understanding the sensitivity of excitable systems to small signals and their robustness to molecular noise in individual cells will help clarify the heterogeneous sensitivity to small chemical gradients for chemotaxis.

Based on our findings, we propose that the highly responsive cells seen in this study promote the initiation of cell aggregation. It has been shown that *Dictyostelium* cells can produce and secrete cAMP stochastically even in the absence of cAMP, and this stochastic secretion is likely to be amplified as the cell density increases [20]. Therefore, the highly sensitive cells observed here can contribute to amplifying extracellular cAMP by gathering in response to stochastic cAMP pulses at the early stages of the wave generation. If this is the case, this minority population can be characterized as highly sensitive to a small number of cAMP molecules to promote the onset of aggregation of the remaining majority of cells. Future analysis of the sub-population sensitive to cAMP below 10^{-10} M may help to characterize the transition from single cells to multicellularity.

Declaration of competing interest

The authors declare that they have no known competing financial interests or personal relationships that could have appeared to influence the work reported in this paper.

Acknowledgments

We would like to thank the National BioResource Project (NBRP)-Nenkin for the *regA*-null strain. We appreciate the information from the DictyBase. We would like to thank P. Karagiannis for critical reading of the manuscript. This work was supported by grants from JSPS KAKENHI Grant Numbers 19H05798 (to S.M.) and 19H00982 (to M.U.). This research was also supported in part by AMED-CREST from Japan Agency for Medical Research and Development, AMED JP20gm0910001 (to M.U.), and PRESTO from Japan

Science and Technology Agency JPMJPR1879 (to S.M.).

Appendix A. Supplementary data

Supplementary data to this article can be found online at https://doi.org/10.1016/j.bbrc.2021.03.095.

References

[1] P. Rørth, Collective cell migration, Annu. Rev. Cell Dev. Biol. 25 (2009) 407–429, https://doi.org/10.1146/annurev.cellbio.042308.113231.

[2] P.N. Devreotes, S. Bhattacharya, M. Edwards, P.A. Iglesias, T. Lampert, Y. Miao, Excitable signal transduction networks in directed cell migration, Annu. Rev. Cell Dev. Biol. 33 (2017) 103–125, https://doi.org/10.1146/annurev-cellbio-100616-060739.

[3] K.J. Tomchik, P.N. Devreotes, Adenosine 3',5'-monophosphate waves in *Dictyostelium discoideum*: a demonstration by isotope dilution - fluorography, Science 212 (1981) 443–446, https://doi.org/10.1126/science.6259734.

[4] H. Hashimura, Y.V. Morimoto, M. Yasui, M. Ueda, Collective cell migration of Dictyostelium without cAMP oscillations at multicellular stages, Communications Biology 2 (2019), https://doi.org/10.1038/s42003-018-0273-6. Article number 34.

[5] P.R. Fisher, R. Merkl, G. Gerisch, Quantitative analysis of cell motility and chemotaxis in *Dictyostelium discoideum* by using an image processing system and a novel chemotaxis chamber providing stationary chemical gradients, J. Cell Biol. 108 (1989) 973–984, https://doi.org/10.1083/jcb.108.3.973.

[6] Y. Kamimura, Y. Miyanaga, M. Ueda, Heterotrimeric G protein shuttling via Gip1 extends the dynamic range of eukaryotic chemotaxis, Proc. Natl. Acad. Sci. U.S.A. 113 (2016) 4356–4361, https://doi.org/10.1073/pnas.1516767113.

[7] T. Miyagawa, H. Koteishi, Y. Kamimura, Y. Miyanaga, K. Takeshita, A. Nakagawa, M. Ueda, M, Structural basis of Gip1 for cytosolic sequestration of G-protein in wide range chemotaxis, Nat. Commun. 9 (2018), https://doi.org/10.1038/s41467-018-07035-x. Article number 4635.

[8] T. Jin, D. Hereld, Chemotaxis, Springer, New York, 2016.

[9] Y. Xiong, C.H. Huang, P.A. Iglesias, P.N. Devreotes, Cells navigate with a local-excitation, global-inhibition-biased excitable network, Proc. Natl. Acad. Sci. U.S.A. 107 (2010) 17079–17086, https://doi.org/10.1073/pnas.1011271107.

[10] Y. Arai, T. Shibata, S. Matsuoka, M.J. Sato, T. Yanagida, M. Ueda, Self-organization of the phosphatidylinositol lipids signaling for random cell migration, Proc. Natl. Acad. Sci. U.S.A. 107 (2010) 12399–12404, https://doi.org/10.1073/pnas.0908278107.

[11] M. Nishikawa, M. Hörning, M. Ueda, T. Shibata, Excitable signal transduction induces both spontaneous and directional cell asymmetries in the Phosphatidylinositol Lipid Signaling System for Eukaryotic Chemotaxis, Biophys. J. 106 (2014) 723–734, https://doi.org/10.1016/j.bpj.2013.12.023.

[12] Y. Miyanaga, Y. Kamimura, H. Kuwayama, P.N. Devreotes, M. Ueda, Chemoattractant receptors activate, recruit and capture G proteins for wide range chemotaxis, Biochem. Biophys. Res. Commun. 507 (2018) 304–310, https://doi.org/10.1016/j.bbrc.2018.11.029.

[13] T.M. Konijn, Microbiological assay of cyclic 3', 5'-AMP, Experientia 26 (1970) 367–369, https://doi.org/10.1007/BF01896891.

[14] J.M. Mato, A. Losada, V. Nanjundiah, T.M. Konun, Signal input for a chemotactic response in the cellular slime mold *Dictyostelium discoideum*, Proc. Natl. Acad. Sci. U. S. A. 72 (1975) 4991–4993, https://doi.org/10.1073/pnas.72.12.4991.

[15] J.A. Swanson, D.L. Taylor, Local and spatially coordinated movements in Dictyostelium discoideum amoebae during chemotaxis, Cell 28 (1982) 225–232, https://doi.org/10.1016/0092-8674(82)90340-3.

[16] P.J. van Haastert, M. Postma, Biased random walk by stochastic fluctuations of chemoattractant-receptor interactions at the lower limit of detection, Biophys. J. 93 (2007) 1787–1796, https://doi.org/10.1529/biophysj.107.104356.

[17] L. Song, S.M. Nadkarni, H.U. Bödeker, C. Beta, A. Bae, C. Franck, W.-J. Rappel, W.F. Loomis, E. Bodenschatz, Dictyostelium discoideum chemotaxis: threshold for directed motion, Eur. J. Cell Biol. 85 (2006) 981–989, https://doi.org/10.1016/j.ejcb.2006.01.012.

[18] Y. Tanaka, K. Sato, T. Shimizu, M. Yamato, T. Okano, T. Kitamori, Biological cells on microchips: new technologies and applications, Biosens. Bioelectron. 23 (2007) 449–458, https://doi.org/10.1016/j.bios.2007.08.006.

[19] H. Moriguchi, T. Kawai, Y. Tanaka, Simple bilayer on-chip valves using reversible sealability of PDMS, RSC Adv. 5 (2015) 5237–5243, https://doi.org/10.1039/c4ra10300a.

[20] T. Gregor, K. Fujimoto, N. Masaki, S. Sawai, The onset of collective behavior in social amoebae, Science 328 (2010) 1021–1025, https://doi.org/10.1126/science.1183415.

[21] M. Brenner, S.D. Thoms, Caffeine blocks activation of cyclic AMP synthesis in Dictyostelium discoideum, Dev. Biol. 101 (1984) 136–146, https://doi.org/10.1016/0012-1606(84)90124-6.

[22] S. Saran, M.E. Meima, E. Alvarez-Curto, K.E. Weening, D.E. Rozen, P. Schaap, cAMP signaling in Dictyostelium. Complexity of cAMP synthesis, degradation and detection, J. Muscle Res. Cell Motil. 23 (2002) 793–802, https://doi.org/10.1023/a:1024483829878.

[23] P.M. Janssens, P.J. Van Haastert, Molecular basis of transmembrane signal transduction in *Dictyostelium discoideum*, Microbiol. Rev. 51 (1987) 396–418.

[24] L. Tweedy, P.A. Thomason1, P.I. Paschke, K. Martin, L.M. Machesk, M. Zagnoni, R.H. Insall, Seeing around corners: cells solve mazes and respond at a distance using attractant breakdown, Science 369 (2020), eaay9792, https://doi.org/10.1126/science.aay9792.

[25] S. Matsuoka, M. Ueda, Mutual inhibition between PTEN and PIP3 generates bistability for polarity in motile cells, Nat. Commun. 9 (2018), https://doi.org/10.1038/s41467-018-06856-0. Article number 4481.

[26] S. Fukushima, S. Matsuoka, M. Ueda, Excitable dynamics of Ras triggers spontaneous symmetry breaking of PIP3 signaling in motile cells, J. Cell Sci. 132 (2019), https://doi.org/10.1242/jcs.224121 jcs224121.

[27] H. Takagi, M.J. Sato, T. Yanagida, M. Ueda, Functional analysis of spontaneous cell movement under different physiological conditions, PloS One 3 (2008) e2648, https://doi.org/10.1371/journal.pone.0002648.

[28] F. Oosawa, Spontaneous signal generation in living cells, Bull. Math. Biol. 63 (2001) 643–654, https://doi.org/10.1006/bulm.2001.0236.

[29] M. Ueda, Y. Sako, T. Tanaka, P. Devreotes, T. Yanagida, Single-molecule analysis of chemotactic signaling in Dictyostelium cells, Science 294 (2001) 864–867, https://doi.org/10.1126/science.1063951.

[30] M. Ueda, T. Shibata, Stochastic signal processing and transduction in chemotactic response of eukaryotic cells, Biophys. J. 93 (2007) 11–20, https://doi.org/10.1529/biophysj.106.100263.

[31] G. Amselem, M. Theves, A. Bae, C. Beta, E. Bodenschatz, Control parameter description of eukaryotic chemotaxis, Phys. Rev. Lett. 109 (2012) 108103, https://doi.org/10.1103/PhysRevLett.109.108103.